

Molecular Gradients of ω -Substituted Alkanethiols on Gold Studied by X-ray Photoelectron Spectroscopy

Bo Liedberg,^{*,†} Mikael Wirde,[‡] Yu-Tai Tao,[§] Pentti Tengvall,[†] and Ulrik Gelius[‡]

Laboratory of Applied Physics, Linköping University, S-58183 Linköping, Sweden, Physics Department, University of Uppsala, S-75121 Uppsala, Sweden, and Institute of Chemistry, Academia Sinica, Nankang, Taipei, Taiwan, Republic of China

Received December 2, 1996. In Final Form: April 23, 1997[⊗]

Molecular gradients of ω -substituted alkanethiols HS(CH₂)₁₅X (X:CH₃, CH₂OH, CO₂CH₃, CH₂C≡N) were prepared on sputtered gold films by using a novel cross-diffusion methodology. Ellipsometry, contact angle measurements, infrared spectroscopy, and X-ray photoelectron spectroscopy (XPS) were used to monitor the coverage, chain conformation and gradient profiles. The XPS analysis were performed with improved lateral resolution as compared to our earlier infrared study (*Langmuir* **1995**, *11*, 3821) by imaging a 160 μ m wide segment of the gradient surface on the slit of the XPS analyzer and by using a step size of 0.5 mm. The so-obtained gradient profiles are expected to be more representative of the true composition profiles and were for the three gradients investigated found to be 5–6 mm, about 2–3 mm shorter than the corresponding profiles obtained by scanning infrared spectroscopy. The coverages (alkyl chain densities) were found to be constant for the gradients prepared from thiols with relatively small tail groups OH, C≡N and CH₃, whereas a minor reduction in coverage, \approx 3–4%, was observed in a narrow range for the gradient containing the CO₂CH₃-terminated alkanethiol. This change is, however, too small to be detected by ellipsometry and infrared spectroscopy and supports a model where the gradient assemblies approach the limiting structure of densely packed all *trans* polymethylenes.

Introduction

Self-assembled monolayers (SAMs) have been thoroughly studied on a variety of solid supports during recent years because of their interesting structural and chemical properties. The increasing demands of well-organized, densely packed, and robust organic surface phases for applications in areas of technological importance such as, micro- and nanopatterning,^{1–4} microelectronics,^{5,6} biochemical and chemical sensing,^{7,8} biomaterials,^{9,10} etc. also have encouraged scientists and engineers outside the academic world to enter the field of self-assembly. So far, the technologically most interesting SAMs have been prepared on oxidic materials like SiO₂ using substituted alkoxy- or chlorosilanes.^{11–13} However, the lack of accurate

protocols for the generation of functionalized and chemically more complex surface phases with predefined and reproducible structures is still a major problem. For example, the role of interfacial water for controlling the growth and formation of highly organized alkylsiloxane assemblies is currently subject to intensive discussions in the literature.^{14–16} The more recent synthetic strategies based on the chemisorption of long-chain organosulfur compounds display many interesting and promising features.^{17–20} In particular, the ability to form so-called mixed SAMs from binary mixtures of ω -substituted alkanethiols HS(CH₂)_{*n*}X/HS(CH₂)_{*m*}Y on gold,^{21–24} with molecular level control over chain conformation, composition, tail group distribution, and mobility, has attracted investigators from diverse areas of material sciences and engineering. Although there is still an active discussion going on in the literature about the exact mechanism by which the thiols(thiolates) chemisorb on the gold surface,^{25,26} as well as about the phase behavior of mixed

* Corresponding author.

[†] Linköping University.

[‡] University of Uppsala.

[§] Academia Sinica.

[⊗] Abstract published in *Advance ACS Abstracts*, September 15, 1997.

(1) Singhvi, R.; Kumar, A.; Lopez, G. P.; Stephanopoulos, G. N.; Wang, D. I. C.; Whitesides, G. M.; Ingber, D. E. *Science* **1994**, *264*, 696.

(2) Lopez, G. P.; Biebuyck, H. A.; Whitesides, G. M. *Langmuir* **1993**, *9*, 1513.

(3) Lopez, G. P.; Albers, M. W.; Schreiber, R. C.; Peralta, E.; Whitesides, G. M. *J. Am. Chem. Soc.* **1993**, *115*, 5877.

(4) (a) Lercel, M. J.; Redinbo, G. F.; Pardo, F. D.; Rooks, M.; Tiberio, R. C.; Simpson, P.; Sheen, C. W.; Parikh, A. N.; Allara, D. L. *J. Vac. Sci. Technol.* **1994**, *B12*, 3663. (b) Lercel, M. J.; Redinbo, G. F.; Rooks, M.; Tiberio, R. C.; Craighead, H. G.; Sheen, C. W.; Allara, D. L. *Microelectron. Eng.* **1995**, *27*, 43–47. (c) Lercel, M. J.; Rooks, M.; Tiberio, R. C.; Craighead, H. G.; Sheen, C. W.; Parikh, A. N.; Allara, D. L. *J. Vac. Sci. Technol.* **1995**, *B13*, 1139–43.

(5) (a) Huang, J.; Hemminger, J. C. *J. Am. Chem. Soc.* **1993**, *115*, 3342. (b) Li, Y.; Hauang, J.; McIver, R. T., Jr.; Hemminger, J. C. *J. Am. Chem. Soc.* **1992**, *114*, 2428.

(6) Huang, J.; Dahlgren, D. A.; Hemminger, J. C. *Langmuir* **1994**, *10*, 626.

(7) (a) Löfås, S.; Johnsson, B. *J. Chem. Soc., Chem. Commun.* **1990**, 1526. (b) Johnsson, B.; Löfås, S.; Lindquist, G. *Anal. Biochem.* **1991**, *198*, 268; (c) Jönsson, U.; Malmqvist, M. *Adv. Biosensors* **1992**, *2*, 291.

(8) (a) Sun, L.; Keply, L. J.; Crooks, R. M. *Langmuir* **1992**, *8*, 2101.

(b) Keply, L. J.; Crooks, R. M.; Ricco, A. J. *Anal. Chem.* **1992**, *64*, 3191.

(9) Tengvall, P.; Lestelius, M.; Liedberg, B.; Lundström, I. *Langmuir* **1992**, *8*, 1236–1238.

(10) Lestelius, M.; Liedberg, B.; Lundström, I.; Tengvall, P. *J. Biomed. Mater. Res.* **1994**, *28*, 871.

(11) (a) Mittal, K. L., Ed. *Silanes and other coupling agents*; VSP: Utrecht, The Netherlands, 1992. (b) Ulman, A. *An introduction to ultrathin organic films: From Langmuir-Blodgett to self-assembly*; Academic Press: San Diego, CA, 1991.

(12) (a) Sagiv, J. *J. Am. Chem. Soc.* **1980**, *102*, 92. (b) Gun, J.; Sagiv, J. *J. Colloid Interface Sci.* **1986**, *112*, 457.

(13) Brzoska, J. B.; Shahidzadeh, N.; Rondelez, F. *Nature* **1992**, *360*, 710.

(14) Brzoska, J. B.; Ben Aazouz, I.; Rondelez, F. *Langmuir* **1994**, *10*, 4367.

(15) Parikh, A. N.; Allara, D. L.; Ben Aazouz, I.; Rondelez, F. *J. Phys. Chem.* **1994**, *98*, 7577–7590.

(16) Parikh, A. N.; Liedberg, B.; Atre, S. A.; Moses Ho; Allara, D. L. *J. Phys. Chem.* **1995**, *99*, 9996.

(17) Nuzzo, R. G.; Allara, D. L. *J. Am. Chem. Soc.* **1983**, *105*, 4481.

(18) Nuzzo, R. G.; Dubois, L. H.; Allara, D. L. *J. Am. Chem. Soc.* **1990**, *112*, 558.

(19) Thoughton, E. B.; Bain, C. D.; Whitesides, G. M.; Nuzzo, R. G.; Allara, D. L.; Porter, M. D. *Langmuir* **1988**, *4*, 365.

(20) Dubois, L. H.; Nuzzo, R. G. *Annu. Rev. Phys. Chem.* **1992**, *60*, 437.

(21) Bain, C. D.; Evall, J.; Whitesides, G. M. *J. Am. Chem. Soc.* **1989**, *111*, 7155.

(22) Bain, C. D.; Whitesides, G. M. *J. Am. Chem. Soc.* **1989**, *111*, 7164.

(23) Bertilsson, L.; Liedberg, B. *Langmuir* **1993**, *9*, 141.

(24) Atre, S. V.; Liedberg, B.; Allara, D. L. *Langmuir* **1995**, *11*, 3882.

SAM,^{27,28} they constitute by far the most well-defined and flexible organic surface chemistry.

We have recently developed a methodology capable of increasing the flexibility of mixed SAMs by forming so-called *molecular gradients* of ω -substituted alkanethiols on gold.^{29,30} The gradients are prepared by cross-diffusing two different alkanethiols from opposite ends of a polysaccharide matrix deposited on top of a gold substrate. The present gradients display many similarities with the gradients formed on Si/SiO₂ by gas or liquid phase diffusion of chlorosilanes^{31–42} and those formed on polymers by using various types of plasma discharge apparatuses.^{43–45} However, the present approach is more flexible in terms of combining different chemical functionalities in the gradient assembly, since it does not rely on having the supporting substrate as one component of the gradient. We are also able to prepare gradients from alkanethiols with different chain lengths, thereby generating an assembly with continuously varying characteristics of the outermost portion of the monolayer, from crystalline-like (*all trans*) at the extreme ends to liquidlike (*gauche rich*) in the intermediate (gradient) region. Our previous study by infrared spectroscopy, ellipsometry, and contact angle measurements suggested that the gradient regions were about 4–8 nm long, depending primarily on the chain length combinations used. The structural properties of the gradients (polymethylene chain conformation, density, and layer thickness) were also found to be almost identical to the corresponding SAMs formed from single component or binary mixtures of ω -substituted alkanethiols.

In this study we report on the characterization of molecular gradients, prepared from ω -substituted alkanethiols of similar chain lengths on sputtered gold surfaces using XPS. A series of gradients prepared from ω -substituted alkanethiols with the general structure HS(CH₂)₁₅X (X = CH₃, CH₂OH, CO₂CH₃, CH₂C≡N) are investigated. The main objective of the study is to determine the *true* gradient and alkyl chain density profiles with improved lateral resolution as compared to our previous scanning infrared and ellipsometric work.²⁹

Experimental Section

Gold Substrates and Chemicals. The gold substrates were prepared by sputter deposition of 200 nm of gold onto glass or silicon substrates primed with 1 nm of chromium. The glass surfaces were precut in different sizes, 4 × 40 mm for XPS, ellipsometry, and contact angle measurements and 20 × 20 mm for IR. The HS(CH₂)₁₆OH and HS(CH₂)₁₅CO₂CH₃ were obtained from BIACORE AB, Uppsala, Sweden (a generous gift from Drs. S. Löfås and B. Johnsson). The 16-cyanoheptadecanethiol (HS-(CH₂)₁₆C≡N) compound was prepared from 16-bromohexadecan-1-ol by first converting it to 16-cyanohexadecan-1-ol via cyanide substitution. Tosylation of the hydroxyl functional group followed by sodium thioacetate substitution and then mild hydrolysis with K₂CO₃ yielded the desired 16-cyanohexadecanethiol, mp 38–39 °C. Finally, HS(CH₂)₁₅CH₃ was purchased from Fluka, Germany. All thiols solutions (2 mM) were prepared in ethanol (95%), by Kemtyl, Stockholm. Other solvents used in this work were of analytical grade and the water was obtained from a MilliQ system (18 MΩ) equipped with an organex filter. Sephadex LH-20, Pharmacia Uppsala, Uppsala, Sweden, was used as the diffusion matrix. This matrix was prepared on top of the gold strips by swelling 3 g of Sephadex LH-20 in 18 g ethanol (95%). After homogenization and evaporation of excess ethanol, the matrix (3–5 mm thick) could be used in the cross-diffusion experiment by injecting the thiol solutions into glass filters placed at opposite ends of the gold strips. A detailed description of the preparation procedure is given elsewhere.²⁹ The diffusion process was interrupted after 48 h, followed by a standard rinsing and sonication procedure in ethanol and water in order to remove the Sephadex LH-20.

X-ray Photoelectron Spectroscopy. The XPS measurements were performed on a Scienta ESCA-300 spectrometer using monochromatized Al K α radiation (1486.6 eV) and a 30 cm (radius) analyzer with a multichannel detection system.⁴⁶ The resolution, as determined from the shape of the Fermi edge of silver using a 0.8 mm slit and 300 eV pass energy, was approximately 0.5 eV. All binding energies given here are referenced against the Au4f_{7/2} peak at 84.0 eV. The statistical error of the integrated intensity of the stronger photoelectron lines (C1s, Au4f_{7/2}) was estimated to be slightly less than $\pm 2\%$, whereas the low intensity lines (N1s, O1s) were expected to exhibit a slightly larger error of about $\pm 3\%$.

Ellipsometry. The ellipsometric measurements were performed with an automatic Rudolph Research AutoEl III ellipsometer. The ellipsometer was equipped with a He–Ne laser ($\lambda = 632.8$ nm) light source and a scanning table (step size of 0.635 mm). The angle of incidence of the laser beam was 70° with respect to the surface normal. A three-layer (parallel slab) model, Au/SAM/air, based on isotropic optical constants for the organic layer, $N_{\text{SAM}} = n + ik = 1.50 + i0$, was used for the evaluation of the gradient thickness.

Contact Angle Measurements. The static liquid drop contact angles with MilliQ water at the very extreme ends of the gradients were measured in a laboratory atmosphere. The contact angle apparatus was equipped with a video camera system developed at our laboratory. At least three droplets were measured directly on the screen of the video monitor, and averaged to represent the correct contact angles within $\pm 2^\circ$.

Infrared Spectroscopy. The infrared reflection-absorption spectroscopy (IRAS) experiments were performed with a Bruker IFS 113v FT-IR spectrometer attached to an in-house customized UHV system equipped with a manual sample scanning and manipulation system. The infrared beam, polarized parallel to the plane of incidence, was aligned at an angle of incidence of 82° with respect to the surface normal and focused on the sample surface using $f/16$ optics.⁴⁷ A narrow band MCT detector was used to detect the light, and 1000 consecutive scans were averaged at 4 cm⁻¹ resolution before Fourier transformation.

Results and Discussion

Table 1 summarizes the ellipsometric, infrared, and contact angle measurements of the three different gra-

(25) Fenter, P.; Eberhardt, A.; Eisenberger, P. *Science* **1994**, *266*, 1216.

(26) Wirde, M.; Gelius, U.; Dunbar, T.; Allara, D. L. *Nucl. Instrum. Methods Phys. Res., Sect. B* **1997**, *130*, 1.

(27) Folkers, J. P.; Laibinis, P. E.; Whitesides, G. M.; Deutch, J. J. *Phys. Chem.* **1994**, *98*, 563.

(28) Stranick, S.; Parikh, A. N.; Tao, Y.-T.; Allara, D. L.; Weiss, P. *J. Phys. Chem.* **1994**, *98*, 7636.

(29) Liedberg, B.; Tengvall, P. *Langmuir* **1995**, *11*, 3821.

(30) Patent pending.

(31) Chaudhury, M. K.; Whitesides, G. M. *Science* **1992**, *256*, 1539.

(32) Elwing, A.; Askendal, A.; Lundström, I. *Prog. Colloid. Polymer Sci.* **1987**, *74*, 103.

(33) Elwing, H.; Welin, S.; Askendal, A.; Nilsson, U.; Lundström, I. *J. Colloid Interface Sci.* **1987**, *119*, 203.

(34) Elwing, H.; Askendal, A.; Lundström, I. *J. Biomed. Mater. Res.* **1987**, *21*, 1023.

(35) Elwing, H.; Welin, S.; Askendal, A.; Lundström, I. *J. Colloid Interface Sci.* **1988**, *123*, 306.

(36) Elwing, H.; Askendal, A.; Lundström, I. *J. Colloid Interface Sci.* **1989**, *128*, 296.

(37) Elwing, H.; Gölander, C.-G. *Adv. Colloid Interface Sci.* **1990**, *32*, 317.

(38) Welin-Klintström, S.; Askendal, A.; Elwing, H. *J. Colloid Interface Sci.* **1993**, *158*, 188.

(39) Hlady, V.; Gölander, C.-G.; Andrade, J. D. *Colloids Surf.* **1987**, *25*, 185.

(40) Gölander, C.-G.; Lin, Y.-S.; Andrade, J. D. *Colloids Surf.* **1990**, *49*, 289.

(41) Hlady, V. *Appl. Spectrosc.* **1991**, *45*, 1991.

(42) Lin, Y. S.; Hlady, V.; Gölander, C.-G. *Colloids and Surf. B: Biointerfaces* **1994**, *3*, 49.

(43) Pitt, W. G. *J. Colloid Interface Sci.* **1989**, *133*, 223.

(44) Lee, J. H.; Kim, H. G.; Khang, G. S.; Lee, H. B.; Jhon, M. S. *J. Colloid Interface Sci.* **1992**, *151*, 563.

(45) Lee, J. H.; Lee, H. B. *J. Biomater. Sci. Polym. Ed.* **1993**, *4*, 467.

(46) Gelius, U.; Wannberg, B.; Baltzer, P.; Fellner-Feldegg, H.; Carlsson, G.; Johansson, C.-G.; Larsson, J.; Münger, P.; Vegerfors, G. *J. Electron. Spectrosc. Relat. Phenom.* **1990**, *52*, 747.

(47) Engquist, I.; Lundström, I.; Liedberg, B. *J. Phys. Chem.* **1995**, *99*, 12257.

Table 1. Ellipsometric, Wetting, and Infrared Data of the Molecular Gradients

monolayer property	gradient					
	ROH/R'CH ₃ ^a		ROH/RC≡N		R'CO ₂ CH ₃ /R'CH ₃	
	OH	CH ₃	OH	C≡N	CO ₂ CH ₃	CH ₃
thickness (Å)	21.5 ± 1	19.5 ± 1	21.5 ± 1	21.0 ± 1	21.5 ± 1	19 ± 1
contact angle $\Theta_{\text{H}_2\text{O}}$ (deg)	<8	112	<8	62	69	112
CH ₂ modes: d ⁻ , d ⁺ (cm ⁻¹)	2919, 2851		c		2919, 2850	
fwhm: d ⁻ , d ⁺ (cm ⁻¹)	16, 11 ^b		c		16, 12	

^a R = SH(CH₂)₁₆; R' = SH(CH₂)₁₅. ^b Typical values reported in the literature for crystalline alkanethiols and bulk *n*-alkanes are as follows. d⁻, 10–13 cm⁻¹; d⁺ 7–10 cm⁻¹.^{18,54} ^c Data not available.

dients investigated in this study. A more detailed examination and interpretation of the ellipsometric, infrared, and contact angle data provided in Table 1 can be found in our previous study.²⁹

Ellipsometry. The ellipsometric thickness obtained from the gradient experiments are all in good agreement with the thicknesses observed for the corresponding single component or mixed monolayers. For example, the HS-(CH₂)₁₆OH/HS(CH₂)₁₅CH₃(OH/CH₃) gradient displays nearly the same thickness variation as the mixed (HS-(CH₂)₁₆OH)_{*f*}/(HS(CH₂)₁₅CH₃)_{1-*f*} monolayers on gold, i.e., from 21 ± 1 Å (*f* = 1) to 19 ± 1 Å (*f* = 0).^{47,48} All gradient profiles show a monotonic change in thickness when going from one extreme side (e.g. OH) via the gradient region into the other extreme side (e.g. CH₃) supporting the generally accepted picture of highly organized and densely packed alkyl chains. However, ellipsometry alone, in this particular case, is not sensitive enough to identify the exact position of the gradient region and its length because of the minor variation in chain length of the investigated diffusion pairs. The molecules used must possess more pronounced differences in either chain length or "bulkiness" of the tail group in order to create a sufficiently large change (contrast) in the measured thickness.²⁹ Spectroscopical techniques are more sensitive to the compositional variations along the substrate surface as will be shown below.

Contact Angle Measurements. The static contact angles with water ($\Theta_{\text{H}_2\text{O}}$), also correspond well to reported values on single component monolayers. Note, however, that the present study only reports $\Theta_{\text{H}_2\text{O}}$ values at the very far (extreme) sides of the gradient assembly. A study on the wettability behavior of the gradients are underway and will be published separately.

Infrared Measurements. The frequencies and full widths at half-maximum (FWHM) of the asymmetric (d⁻) and symmetric (d⁺) methylene stretching modes are also given for two of the gradients in Table 1 since they can provide valuable information about the polymethylene chain conformation.^{49–52} The d⁻ and d⁺ frequencies are all very close to those reported for the corresponding single component and mixed monolayers. For example, Engquist et al. reported d⁻ values between 2917.7 and 2919.3 cm⁻¹ for mixed (HS(CH₂)₁₅OH)_{*f*}/(HS(CH₂)₁₅CH₃)_{1-*f*} (0 < *f* < 1) monolayers⁴⁷ and at 2919 cm⁻¹ for a pure HS(CH₂)₁₅-CO₂CH₃ monolayer.⁵³ Thus, the intra chain structure of the gradients approaches the limiting case of conforma-

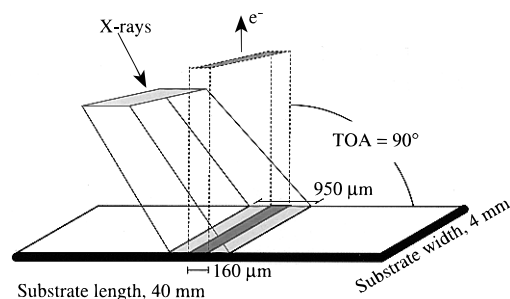


Figure 1. Experimental geometry used for obtaining the XPS gradient profiles. A 160 μm × 4 mm large area of the substrate is imaged on the entrance slit of the XPS analyzer. The step size was 0.5 mm, and the take off angle (TOA), defined as the angle between the plane of the gold substrate and the analyzer slit, was 90°.

tionally ordered all *trans* alkyl chains of similar quality as mixed alkanethiolate SAMs. The upward shift of the d⁻ mode (≈ 1 cm⁻¹) as compared to the very best single component SAMs may indicate a partial disordering of the alkyl chains. However, since the shift is very small, we feel that it is reasonable to assume that the conformationally disordered (*gauche*) components are preferentially localized at the outermost portion of the monolayers. The full width of half maximum (FWHM) of the d⁻ and d⁺ modes are larger in the gradient spectra, typically 4 and 2 cm⁻¹, respectively, as compared to the corresponding modes in the spectra of the very best alkanethiolate SAMs supporting what already has been said about a slight increase in the population of *gauche* conformers in the gradient assemblies.

Altogether the ellipsometric, IR, and contact angle measurements suggest that the gradient assemblies consist of dense and highly organized polymethylene chains of almost the same internal structure and quality as the single component or mixed monolayers. A drawback with the infrared and ellipsometric analyses is, however, that the spot sizes typically fall in the millimeter range. Such large spots will effectively smear out the gradient profiles and make them to look longer than they actually are. In this paper we address this issue in detail by performing XPS experiments with substantially improved lateral resolution.

X-ray Photoelectron Spectroscopy. X-ray photoelectron spectroscopy is utilized to study the lateral composition and coverage (density) of the gradients. The experimental geometry used is schematically illustrated in Figure 1. The photoelectrons are analyzed at a take-off angle (TOA) of 90° with respect to the plane of the surface. A 160 μm wide and 4 mm long (the width of the gold substrate) area is imaged on the entrance slit of the hemispherical analyzer, and the step size between each analyzed area is 0.5 mm. This step size is chosen to minimize the exposure time of the X-ray radiation on the monolayer prior to analysis because recent studies have shown that the gold–thiolate bond is sensitive to prolonged exposure to X-ray radiation.²⁶

(48) Parikh, A. N.; Liedberg, B.; Atre, S. V.; Ho, M.; Allara, D. L. *J. Phys. Chem.* **1995**, *99*, 9996.

(49) MacPhail, R. A.; Strauss, H. L.; Snyder, R. G.; Elliger, C. A. *J. Phys. Chem.* **1984**, *88*, 334.

(50) Snyder, R. G.; Strauss, H. L.; Elliger, C. A. *J. Chem. Phys.* **1982**, *86*, 5145.

(51) Snyder, R. G.; Maroncelli, M.; Strauss, H. L.; Hallmark, V. M. *J. Chem. Phys.* **1986**, *90*, 5623.

(52) Snyder, R. G. *Macromolecules* **1990**, *23*, 2081.

(53) Engquist, I.; Lestelius, M.; Liedberg, B. *J. Phys. Chem.* **1995**, *99*, 14198.

(54) Wood, K. A.; Snyder, R. G.; Strauss, H. L. *J. Chem. Phys.* **1989**, *91*, 5255.

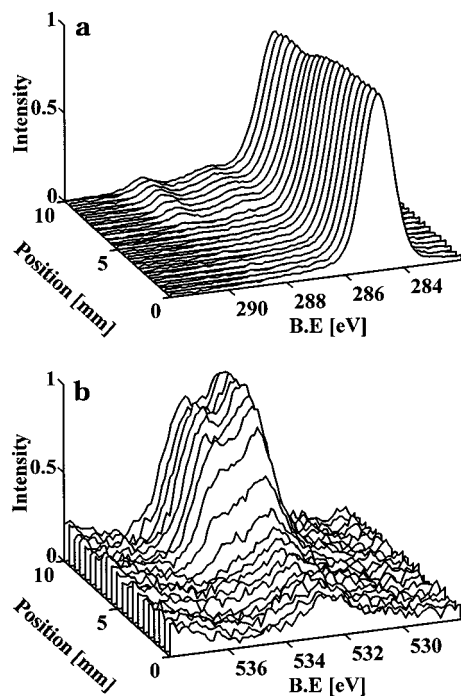


Figure 2. Stacked plots of the (a) C1s (282–292 eV) and (b) O1s (528–538 eV) peaks obtained from the HS(CH₂)₁₅CO₂CH₃/HS(CH₂)₁₅CH₃ gradient assembly.

Figure 2 shows stacked plots of the C1s and O1s core level XPS spectra for the HS(CH₂)₁₅CO₂CH₃/HS(CH₂)₁₅CH₃ (CO₂CH₃/CH₃) gradient as a function of position. The C1s spectra, Figure 2a, display three well-resolved peaks at 284.8, 286.8 and 289.3 eV, respectively. The 284.8 eV peak is due to the methylene –CH₂– carbons in the alkyl chain. The two chemically shifted peaks at 286.8 and 289.3 eV are attributed to the –OCH₃ and C=O (carbonyl) carbons of the tail group, respectively. Two additional, less well-resolved, peaks originating from the tail group are also observed in the curve fitting analysis at 285.4 and 287.8 eV. The binding energies as well as the relative intensities of the C1s peaks are in good agreement with the corresponding peaks of the single component HS(CH₂)₁₅CO₂CH₃ and HS(CH₂)₁₅CH₃ SAMs suggesting that the gradient assembly is free from organic contamination. It should be emphasized, however, that the diffusion matrix, Sephadex, adhered quite strongly to the (CO₂CH₃/CH₃) gradient. It was therefore, necessary to develop a special cleaning protocol for this gradient to ensure that no Sephadex was left on the surface. This cleaning protocol includes the standard procedure, i.e., extensive rinsing in ethanol and water followed by ultrasonication for 5 min in ethanol and water, plus sequential ultrasonication for 5 min in each of the following solvents: carbon tetrachloride, acetone, 2-propanol, and water. Figure 2b shows the evolution of the two O1s peaks as we move along the gradient. The peak at 532.5 eV is attributed to the C=O(carbonyl) oxygen and the peak at 534.0 eV to the single bonded –OCH₃ oxygen. Also seen in Figure 2b is a small peak near 532.5 eV which becomes clearly visible when moving into the far CH₃ side of the gradient (pos → 0 mm). This peak is most likely due to adsorbed water, and it appears on all gradients, though with different intensities depending on the surface energy (cos Θ_{H₂O}) as well as on the number of cleaning cycles with water used for removing the Sephadex matrix. The large number of cleaning steps employed to remove Sephadex from the gradient surface may explain the presence of this peak. The water O1s peak is also present on the methyl ester side of the gradient as revealed by the deviation from the

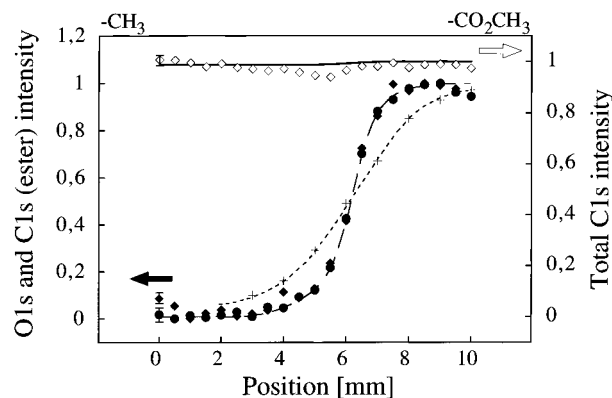


Figure 3. XPS intensity profiles obtained from the stacked plots of the HS(CH₂)₁₅CO₂CH₃/HS(CH₂)₁₅CH₃ gradient in Figure 2: (●) O1s intensity; (◆) C1s(ester), obtained from the sum of the peak intensities of the four chemically shifted C1s peaks; (◇) total C1s intensity (282–292 eV); (–) semiempirical total C1s intensity; (+) infrared C=O gradient profile, replotted from data from Figure 6a, in ref 29. The lines through (●) and (+) should only be regarded as guide lines for the eye. The error bars show the estimated statistical errors in the integrated intensities. A special cleaning procedure involving carbon tetrachloride, acetone, and 2-propanol was used for this gradient.

expected 1:1 relative intensity ratio for the 532.5 and 533.9 peaks. The water peak in the first spectrum (pos = 0 mm) is therefore subtracted from all spectra, pos > 0 mm, prior to integration and calculation of the gradient profiles; see below. To subtract a constant factor from all spectra is of course questionable and must be regarded as a first-order approximation, since a CO₂CH₃ surface (intermediate surface energy) is expected to be more prone to keep a thin layer of water than a hydrophobic (low energy) surface.⁴⁸

The normalized C1s and O1s integrated intensities, determined after a proper base-line correction and curve-fitting procedure, are plotted in Figure 3 to represent the gradient profiles. As expected, the O1s (●) and C1s (◆) peak intensities, the latter based on the sum of the individual peak intensities of the four chemically shifted peaks (285.4, 286.8, 287.8 and 289.3 eV) follow very nicely the same trend. Both profiles indicate that the gradient region is about 5 mm long. Also shown in Figure 3 is the profile obtained from scanning infrared spectroscopy (+), by integrating the C=O stretching band near 1746 cm⁻¹ (replotted from Figure 6a, ref 29). The profiles determined from the two methods are different. The IR-profile display a smoother, less steep, change with position along the gradient, and the corresponding length determined by IR is approximately 8 mm. This difference in length is actually not unexpected since the spot size used in the IR setup is at least 1 order of magnitude larger than the one used in the present XPS experiments. Thus, our previous hypothesis that the IR measurements most likely overestimate the gradient lengths²⁹ is clearly confirmed by the present XPS results. We therefore conclude that the 5 mm obtained here should be regarded as a more representative value of the *true* length of the CO₂CH₃/CH₃ gradient. It should also be emphasized that XPS, in general, is a more reliable method than IR for compositional analyses, since not only the composition but also the molecular orientation with respect to the metal surface will contribute to the intensity in the IRAS spectrum.¹⁸

Another important property for the stability and future application of the gradient assemblies is the coverage and the packing density of the alkyl chains. We have in this study used the total C1s intensity as a measure of the

variation in coverage (density) along the gradient. The so-obtained profile is compared with the semiempirical profile derived from the actual gradient profile (●) and estimated attenuation factors of the heteroatoms in the various tail groups.⁵⁵ The expression for the attenuated intensity of the C1s photoelectrons from the all *trans* alkyl chains tilting with an angle τ from the surface normal is given by

$$I = \frac{I_0(\tau)}{\sin \theta} \sum_{\substack{k=1 \\ \text{only C} \\ \text{atoms}}}^N \exp \left\{ - \sum_{n=k}^N \frac{\Delta x_n(\tau)}{\lambda_n \sin \theta} \right\} \quad (1)$$

where N is the total number of non-hydrogen atoms in the molecule. I_0 is the C1s intensity recorded from one unattenuated layer of $-\text{CH}_2-$ units at TOA = 90° . θ is the actual TOA used. $\Delta x_n(\tau)$ is the distance between two neighboring layers n and $n+1$, except for $\Delta x_N(\tau)$, which is by definition set to zero since there is no attenuating layer above layer N . The heteroatoms of the tail groups are also included in the sum in the exponent. Generally, the attenuation lengths λ_n should vary with layer density and atomic species within each layer, but here a constant λ has been used, even for the end group heteroatoms. The value of λ , in our case 35 Å, is calculated from the empirical parametrization given by Laibinis et al.⁵⁶ The layer distances are chosen from a generally accepted model where the alkyl chains tilt at $\tau = 29^\circ$, giving $\Delta x_n(29^\circ) = 1.10 \text{ \AA}$ for $n < N$.

The total integrated C1s intensity (282–292 eV) is plotted in Figure 3 (◇) together with the semiempirical profile for the total C1s intensity, the fat solid line. The experimental profile agrees well with the theoretical one at the extreme CH_3 and CO_2CH_3 sides of the assembly, but deviates slightly between 5 and 6 mm, close to the onset of the gradient region. This decrease may in part be due to inaccurate modeling of the various factors influencing the attenuation of the photoelectrons. Another plausible explanation is that the alkyl chains are less densely packed in this particular part of the gradient region. A lower density, surface coverage, will inevitably perturb the alkyl chain conformation near an empty spot and thus increase the population of *gauche* conformers. Our previous infrared results²⁹ do not provide any supporting evidence for an increased conformational disordering of the alkyl chains, the d^- frequency remain constant throughout the entire gradient region. Nor can we observe any drop in the ellipsometric thickness in the gradient region. Thus, XPS seems to be a far more sensitive technique than both ellipsometry and IR for monitoring the variation in surface coverage (density). However, the decrease in surface coverage is still expected to be fairly small. The deviation from the theoretical profile between 5 and 6 mm $\approx 3\text{--}4\%$ would mean that about one of 25–33 thiols is missing, a reduction which in a first-order approximation is expected to correspond to about 0.65–0.85 Å in the ellipsometric thickness ($1/33 - 1/25$ of the film thickness), i.e., a change within the error limits of the ellipsometric analysis. It is more difficult to foresee how a 3–4% reduction in coverage will influence, for example, the d^- mode frequency and line shape. We merely conclude that the effect must be fairly small since no shift can be seen in the IR spectra recorded along the gradient.²⁹

(55) Supplementary material describing the method used for calculating the semiempirical gradient profiles is available from the author upon request.

(56) Laibinis, P. E.; Bain, C. D.; Whitesides, G. M. *J. Phys. Chem.* **1991**, *95*, 7017.

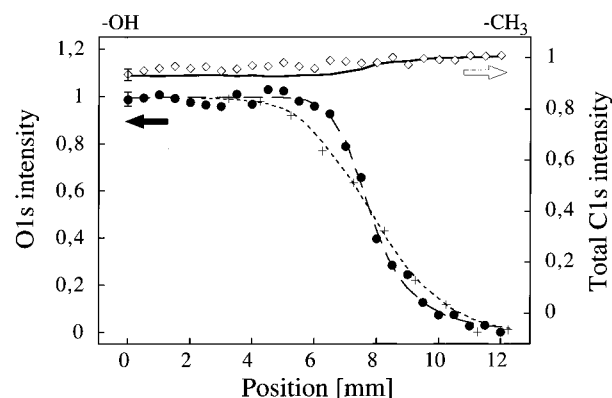


Figure 4. XPS intensity profiles obtained from the $\text{HS}(\text{CH}_2)_{16}\text{-OH}/\text{HS}(\text{CH}_2)_{15}\text{-CH}_3$ gradient. (●) O1s intensity; (◇) experimental total C1s intensity (282–292 eV); (—) semiempirical total C1s intensity; (+) infrared gradient profile obtained from the integrated ν^- peak intensity. The lines through (●) and (+) should only be regarded as guide lines for the eye.

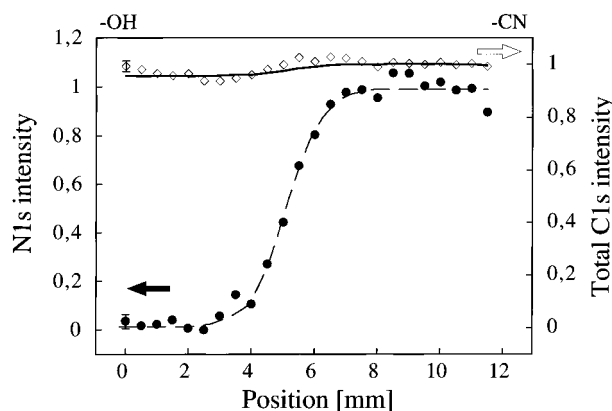


Figure 5. XPS intensity profiles obtained from the $\text{HS}(\text{CH}_2)_{16}\text{-OH}/\text{HS}(\text{CH}_2)_{16}\text{-CN}$ gradient. (●) N1s intensity; (◇) experimental total C1s intensity (282–292 eV); (—) semiempirical total C1s intensity. The lines through (●) should only be regarded as a guide line for the eye.

Figure 4 shows the gradient profile for the (OH/CH₃) gradient. The integrated intensity of the O1s peak at 532.6 eV is used to generate the profile (●). Also plotted in Figure 4 is the gradient profile from scanning infrared spectroscopy obtained by integrating the ν^- , $\nu_{\text{as}}(\text{CH}_3)$, mode near 2964 cm^{-1} (+). Again, we find a smoother appearance of the profile obtained by IR. The IR experiments also overestimate the length of the gradient, 7–8 mm, as compared to the 5.5–6 mm obtained with XPS. The total C1s intensity (282–292 eV) display a monotonic decrease when moving from the CH_3 - towards the OH side (◇). This behavior is consistent with a gradual increase in the attenuation of the C1s photoelectrons by the terminal hydroxyl group. However, no evidence whatsoever can be found for a decreasing coverage in the gradient region.

Similarly, the N1s (●) profile of the (OH/CN) gradient is shown in Figure 5. It is based on the integrated intensity of the N1s peak at 400.0 eV. Again we estimate the gradient length to be about 5.5 mm. The total C1s intensity (◇) increases when passing the gradient from the OH to the CN side. This increasing C1s intensity is in good agreement with the increase in the total number of carbon atoms in the OH and CN thiols, respectively. The semiempirical curve displays the same trend, confirming our picture of densely packed assemblies throughout the gradient region.

The present XPS analyses reveal that the IR overestimates the lengths of the gradients a result of which is of importance for future applications. We believe also

that the gradient assemblies are attractive model organic interfaces, and more detailed investigations concerning their microscopic wetting properties using water (ice) as the probing liquid (adsorbate) are currently underway. Order-disorder gradients prepared from *n*-alkanethiols of different chain lengths have also been prepared and currently analyzed with scanning liquid drop contact angle measurements and IR.

Conclusions

Molecular gradients prepared from ω -substituted alkanethiols with approximately the same chain lengths, 15 and 16 methylene units, and the following combinations of tail groups CO₂CH₃/CH₃, OH/CH₃ and OH/CN, have been analyzed with X-ray photoelectron spectroscopy. The analyses are performed with improved lateral resolution as compared to our earlier infrared characterization,²⁹ to yield the *true* gradient profiles (lengths). All gradients are determined to be 5–6 nm long, i.e., about 2–3 nm shorter than the lengths observed with scanning infrared spectroscopy. This shortening was in fact predicted in our previous infrared study²⁹ and is entirely due to the smaller spot size used in the XPS analysis. The coverages (alkyl chain densities) observed for the OH/CH₃ and OH/CN gradients, as determined from the total C1s intensity profiles, are consistent with the formation of densely packed all *trans* polymethylene chains, an observation in excellent agreement with infrared and ellipsometric findings.²⁹ A small \approx 3–4% reduction in coverage is

observed in the gradient region for the CO₂CH₃/CH₃ gradient. This loss of molecules is, however, too small to be detected as a change in the ellipsometric thickness as well as a shift in the frequencies of the methylene stretching modes in the infrared spectra. A brighter and smaller spot size for the infrared analysis would certainly help addressing the above issues with improved lateral resolution.

Finally, the approach used to prepare molecular gradients of ω -substituted alkanethiols seems very promising for a wide range of applications in surface chemistry and materials sciences. We have so far only employed thiols with relatively simple tail groups. However, more complex thiols are currently investigated and the results will be published separately. We are also investigating the possibilities of using the alkanethiol gradients as templates for the generation and growth of more complex supramolecular architectures and as models for the optimization of the interfacial properties of biomaterials and biosensor surfaces.

Acknowledgment. This research was supported by grants from the Swedish Research Council for Engineering Sciences (TFR) and from the Swedish National Board for Technical and Industrial Development (NUTEK) and the Swedish Natural Science Research Council (NFR) through the Swedish Biomaterials Consortium.

LA962053T